Proc. of the 11th International Symposium on Long Range Sound Propagation , 2-3 June 2004, Fairlee, VT, USA.

A Field Trial on the Influence of Range-Dependent Meteorology on Outdoor Sound Propagation

Y. W. Lam and D. C. Waddington
Acoustics Research Centre, University of Salford, Salford M5 4WT, UK
Tel: +44 161 295 4989 Fax: +44 161 295 5145.
E-mail: y.w.lam@salford.ac.uk

ABSTRACT

This paper reports on the findings of a field trial programme to investigate the effect of range-dependent meteorology on sound propagation in the atmosphere. Comparisons are made with predictions derived from a PE model utilising the range-dependent meteorology and terrain data derived from the field trail. An experiment is described in which range-dependent meteorological and acoustical data were simultaneously measured during the onset of stable nighttime conditions. A Doppler LIDAR measured winds in scans above the length of the 1km acoustical array rising from the bottom of a valley. Vertical winds, temperatures and turbulence were determined in a column at one point on the array by a combined SODAR, RASS and sonic anemometer system. Wind profiles were also measured using a SODAR positioned 250 metres along the receiving array within the valley. Experimental results are presented investigating the effects of variable meteorology on propagation with distance, and significant intermittent episodes of depressed and elevated sound levels are considered.

I. INTRODUCTION

It is well known that the ground and the atmosphere have large influences on how sound propagates outdoors. The influences tend to grow larger at longer ranges but even at short to medium ranges the effects can still be substantial. In recent years there have been many studies into and much improved knowledge on how the ground and the atmosphere should be modelled and incorporated into various outdoor sound propagation prediction schemes. For examples, it is now known that the simple 1 parameter ground impedance model based on the empirical results of Delaney and Bazley **[1]** is not adequate in certain situations and more sophisticated multi-parameter models **[2]** can give better predictions over a wider range of conditions. As for the atmosphere, it is clear that the vertical sound speed profile is far from a simple linear or even a logarithm one and a simple 1 dimensional, isotropic Gaussian model may not be adequate for modelling the true turbulence spectrum **[3,4,5]**.

With this improved knowledge, there is an increasing demand into more detailed and accurate ground and atmospheric data to be fed into acoustic models. Yet there are very few comprehensive field data available that would allow one to perform acoustic predictions with fully characterised ground and atmosphere conditions. In most cases, ground data is still estimated from typical, best guessed values based on the

appearance of the ground cover. Atmospheric data, in terms of wind and temperature, are either measured by fixed location sensors mounted on masts no higher than 30m or snap-shot high atmospheric data obtained from radiosone. In almost all cases the range dependence of the data is not available since they are not measured. This is rather surprising especially for long range sound propagation studies since one would expect the ground and the atmosphere to change significantly over a long range.

The field trial reported here has two aims. Firstly it was set up to test if reliable and sufficiently detailed atmospheric data can be obtained from remote sensing atmospheric measurement devices to improve acoustic prediction accuracy. Sodar, which is an audio signal based remote sensing device used to scan wind profiles vertically, has been available for a long time. Modern Sodar also has the capability to derive temperature data from a RASS system, and there are also mini-Sodar systems that can be mounted on a trailer and be transported to locations easily. More recently remote sensing based on laser technology has also become available in Lidar systems **[6]**. The Lidar also offers the opportunity to scan both horizontal and vertical directions and thus can in theory provide very detailed range dependent vertical wind profiles. The potential problem of these remote sensing technologies is that the atmospheric data are derived from very low level back scattering of sound from air turbulence (Sodar), or back scattering of light from tiny air particles (Lidar). With such low level signals the potential error in the extract of atmospheric data from these devices could be significant. The first objective of the field trial is therefore to see if the atmospheric data obtained from these remote sensing devices can provide a good prediction of the sound propagation results.

The second object is to see if the range dependence in ground and atmospheric data is an important factor in sound propagation. Obviously the investigation here is limited by the available sensors and locations. To improve our chance of success, the field trial was conducted in a site that has a range varying terrain. Two Sodar systems were deployed at different locations along the propagation path to track the changes in the wind profile and a Lidar system was used to scan the vertical wind profiles at different horizontal ranges. As for the ground, in-situ ground impedance measurements **[7]** were conducted at different locations. All in all this represents the most comprehensive data set that we could afford to measure.

The acoustic propagation data were measured at synchronised time intervals with the meteorology measurements. Predictions of the sound propagation were carried out by means of a GTPE **[8]** implementation. Since the ground terrain has some sharp changes in the geometry, which may cause problems for the GTPE, predictions were also done using a 2D boundary integral equation method (BEM) method **[9]** for the still air case to provide a reference for comparisons. All in all 4 days of measurements were carried out and this paper reports on the findings on one of the 24-hour periods, from 22:00 21 August 2002 to 22:00 22 August 2002, in which the measured data are most completed.

II. THE FIELD TRIAL SITE

The site is located in a shallow valley with the main measurement/propagation direction along a gentle slop rising to about 90m height over a range of 1100m and then drops back again at a gradient of about 2 in 10. A microphone was placed behind

the hill top to test barrier and turbulence effects created by the hill top at a fairly long range. Besides the largely gentle slope there is a rather sharp, 3m ditch at around 250m. Perpendicular to the main propagation direction the terrain also rises up by about 35m over a 300m horizontal distance. Microphones were also placed cross-valley for future references. The terrain was surveyed using a high grade GPS system with an accuracy of about ±1m at about every 20m if accessible. The valley terrain was thought to be likely to create range dependent effects in the ground and meteorology data.

The ground cover near the source was soft with short to medium grass, fairly flat for the source and associated equipment to be mounted. From about 300m the ground changes to a boggy cover with meter long grass. Approaching the hill top the ground turns harder with short grass.

A total of 4 days of measurements were carried out between 19 August to 22 August 2002. The weather was mainly dry and cloudy with light wind (below 5m/s at 10m height). We would have liked to have stronger wind conditions but unfortunately we could not control the weather.

III. MEASURMENTS

(A) Acoustic Measurements

The main line of sound propagation measurement was from East to West along the slope of the valley. The source was located at the bottom of the valley and the base of the source is designated as range x=0. Microphones were placed at locations as shown in Figure 1 and the furthest is at 1179m west of the source behind the hill top. The acoustical field trial data was prepared from Type 1 measurements made by acoustical monitoring units with a microphone height of 1.5m installed at approximately 112m intervals along the main propagation path and approximately 75m intervals cross-valley. Additional reference positions were installed at 10m from the sound source in order to monitor any source power fluctuations. Each station was used as a stand-alone data logger recording L_{eq} and 1/3 octave band spectra each second. In the analyses these data have been averaged over 150s time periods synchronised with Lidar and Sodar measurements of wind and temperature profiles. The sound source emitted pink noise in cycle consisting of 15 second ramp-up, five-minute source-on, 15 second ramp-down, and 30 seconds of silence to enable background levels to be monitored. The acoustical L_{Aeq} (150s) were calculated for source-on times only with allowance made for background noise. Measurements <7dB above background noise in the closest time interval were discarded. On each day the measurement nominally started at around 22:00 and ran through to 22:00 of the next day, with some gaps in between for data backup and equipment re-calibration.

To minimise the uncertainty in source characteristics, an omni-directional (within ±3dB in the operational frequency range) dodecahedron loudspeaker source driven by a modified Maximum Length Sequence pseudo-random signal was used. The nominal maximum sound power level (SWL) from the source was 120dB with a frequency range of 100Hz to 4kHz. In the field the SWL achieved was 105-115dB within each 1/3 octave bands from 125Hz to 3kHz when driven by a mobile diesel engine power generator. The power output fluctuates within ±2.5dB during the trial. This is

compensated by the levels measured at the monitor microphones at 10m from the source. The centre of the source is at a height of 2m from the ground.

(B) Ground Impedance Measurements

Ground impedance was deduced from measurements of short range excess attenuation spectra at three locations along the main propagation path. One is near the source, the other in the middle and the last one near the hill top. The three locations had visually very different appearances. Three different source and receiver heights, from 10cm to 30cm were used at each location, and usable spectra were visually selected for the best fit procedure. The deduced impedance spectra were used to best fit ground parameters using both the 1 parameter Delaney and Bazley model **[1]** and the 2 parameter ground model **[2]**. Figure 2 shows typical fits to one of the impedance spectra. Overall the 2 parameter model gave better fits to the impedance over the frequency from 500Hz to 2 kHz. The resulting best fit parameters, averaged over all the measurements at different heights at each location, for the two models at the three ground measurement locations are summarised in Table 1.

Table 1 Parameters for the Two Ground Models at 3 locations in the Field Trial.

Position	2 Parameter Ground Model		Delaney & Bazley
	Effective flow resistivity σ (kPa/m^2)	Effective rate of change of porosity α_e (/m)	Effective flow resistivity σ (kPa/m^2)
Near source	10	68	60
At 500m	23	124	124
At 975m	23	-84	43

Since the 2 Parameter ground model gave better fit to the measured data, it was used in all subsequent predictions that are presented later in this paper.

(C) Meteorology Measurements

Since one of the main objectives of the field trial is to study the meteorology influences on sound propagation, a large range of meteorology measuring equipment was deployed. This includes:

1. A Lidar system – a remote sensing laser Doppler radar that can scan vertical wind speed profiles at horizontal intervals of approximately every 100m up to a range of 4km. Accuracy is still being verified.
2. A Metek Sodar with a RASS system – a remote sensing sound radar that scans vertical wind speed, wind direction, and temperature profiles from a height of about 129m to 600m. The nominal accuracy is claimed to be ±0.2m/s, ±5º, and ±5ºC.
3. An Aerovironment (AES) Sodar - a mini remote sensing sound radar that scans vertical wind speed and wind direction profiles from a height of about 15m to 300m. The nominal accuracy is claimed to be ±0.5m/s and ±5º.
4. A Metek sonic anemometer and temperature sensor that could be used to derive 1 dimensional isotropic turbulence parameters. The nominal accuracy is claimed to be ±0.2m/s, ±5º, and ±5ºC.

5. A typical environmental weather monitoring rotating vane anemometer and temperature sensor.

The Lidar is still an experimental device that is constantly under development. Its main advantage over all others is the ability to scan both horizontal and vertical wind speed profiles and is therefore a convenient device for range dependent studies. It is however highly sensitive to the amount of back-scattering particles in the air and cannot be operated at all times. Subsequently usable Lidar data were obtained only on one of the 4 days of measurements. The Lidar is mounted in a mobile van and requires a flat location to operate. It also has a requirement of an initial distance of 600m before the first scan. During the field trial it was located about 700m east of the source so that the scans covered the whole propagation path west of the source. This location is however about 30m higher than the source location which is at the bottom of the valley. Additionally the laser had to be tilted slightly upwards to avoid reflection from the slope of the valley. Subsequently not all the lower heights were covered by the scans.

The Metek Sodar and RASS system is rather large and needs to be installed over a large, flat and hard surface. The only suitable location at the site was on the hill top near the furthest microphone position at about 1100m west of the source. Since the Metek scans start from a height above 100m, a sonic anemometer and temperature sensor were also mounted near the Sodar at a height of 10m to provide lower height meteorology data. The sonic anemometer also has a fast enough response time to allow extraction of turbulence structure parameters based on a 1 dimensional isotropic turbulence model.

The AES Sodar is a mini, "portable" Sodar that is mounted on a trailer. Its placement is therefore more flexible. During the field trial it was placed at about 400m west of the source. Due to the boggy ground along the propagation path, it was placed at a lateral offset of about 50m on a dry, hard surface. The small size of the AES Sodar limits the maximum scan height to about 300m but at the same time allows scans to start at a height as low as about 15m. There is no RASS system with this Sodar and therefore only wind profiles were obtained from it.

The remaining environmental weather station was mounted near the source with the anemometer and temperature sensor on a mast at 2m to provide nominal monitoring of the weather. Unfortunately with only one sensor location it is not possible to derive vertical wind or temperature profiles reliably from this weather station.

IV. MEASURED DATA

(A) Acoustic Data

Acoustic data were obtained on all 4 days of measurements in L_{Aeq} and 1/3 octave bands from 50Hz to 10kHz. Only data that are 7dB above background noise level were selected and stored into a database. Although the source is powerful enough to provide a L_{Aeq} of about 90 dB(A) at 10m from the source, the presence of ground attenuation and terrain screening effects reduce the signal levels at several microphone positions considerably and a lot of the 1/3 octave band data did not meet the signal to noise level criterion and had to be discarded. Nevertheless the database

still contains a large amount of usable data, sufficient for our investigation into the ground and meteorological effects.

Over the field trial, the source power fluctuated within about ±2.5dB over all 1/3 octave bands within the usable frequency range of 100Hz to 3 kHz. The variation was recorded by the monitor microphones at 10m from the source and was corrected for in the predictions. Figure 3 shows the measured sound propagation at 200Hz and 500Hz along the main propagation path west of the source. The dataset is labelled "020821" which corresponds to data from the 24 hour cycle from 22:00 on 21 August 2002 to 22:00 22 August 2002. This dataset will be used throughout this paper. The figure also shows the calculated free field values that are adjusted for source power fluctuations. The result in the 200Hz band clearly shows the considerable drop in mean SPL due to ground attenuation throughout the day. While in the 500Hz band, where sound levels have largely recovered from the ground attenuation, the spread of levels due to meteorology and the attenuation due to terrain screening at the 250m and 1179m microphone positions can be clearly seen. Figure 5 shows the variation of the L_{Aeq} over the 24 hour period of the dataset at the 501m microphone position. Significant variations of the sound level over different time of the day can be seen. The acoustic data from the field trial contain features showing the effects of ground terrain and meteorology over the 1.2km range.

(B) Wind and Temperature Profiles

The meteorology and acoustic data are time synchronised and averaged into 150s time bins so that the two sets of data can be directly correlated. An overview of the vector wind data derived by the Metek Sodar and the Lidar scan at the corresponding position of 1100m west of the source is shown in Figure 5(a) while a similar overview of the AES Sodar and Lidar data at 428m west of source is shown in Figure 5(b). Note that the Lidar scans in time bins of 150s interval contain errors too large to be usable. It is necessary to perform averages over 10 minutes to obtain usable data. The figure therefore shows Lidar data that were averaged into 10 minute intervals. In later sections of this paper, predictions using Metek and AES Sodar data are still based on 150s data unless otherwise specified, while predictions using Lidar data are based on 10 minute averages.

Although there are variations within and between the different sets of data, the figure shows that the general trends of the profiles are compatible and tend to follow each other, largely within ±1m/s, except those from the AES Sodar which show stronger gradients at the lower heights. The vector wind speeds from all measurements are largely below 2m/s at heights below 10m and confirm the impression that the wind was very light on that day of the measurement. Overall there is reasonable agreement between the different data sets but the accuracy of the Lidar data in short time frames is still a concern.

There is only 1 set of temperature profile data obtained from the Metek RASS system. An overview of the data is shown in Figure 6. Note that the data points at 10m are added from the temperature sensor measurements from the Metek sonic anemometer. The temperature profiles show strong gradients at low vertical heights.

(C) Turbulence

Since only one sonic anemometer was used in the trial, only parameters for a 1 dimensional isotropic turbulence model can be derived. An analysis of the full turbulence structure is still on going. Figure 7 shows the results of a limited analysis over a 3.3 hour period. Although all the data has not been fully analysed, the preliminary results show rather small turbulence strength. Further wok will need to be done to fully appreciate the data.

V. PREDICTIONS

The main prediction tool used in this study is an implementation of the general terrain parabolic equation (GTPE) **[8]**, which can handle a smooth undulating ground terrain and range dependent ground impedance and meteorology profiles. In the GTPE calculations, sound pressures were calculated at 1/6 wavelength intervals and then averaged over approximately 1m to provide the output. Initially there was concern about the impact of the sharp changes in the terrain geometry on the accuracy of the GTPE. Hence a 2 dimensional boundary integral equation method (BEM) **[9]** was also used to calculate the sound propagation under still air condition. The BEM models the entire ground terrain from the source to the furthest receiver using small boundary elements, and can handle impedance and sharp terrain changes without losing accuracy. With its good accuracy, the BEM can be used as a reference to validate the GTPE prediction under still air condition. Additionally it will be more precise to use the BEM to investigate the effect of range dependent ground impedance without the influence of meteorology. To keep the BEM model to a reasonably small size the ground was assumed to be hard beyond 100m from either ends of the propagation path so that symmetry can be used to model the hard ground.

(A) Range Dependent Ground

Figure 8 shows the BEM predictions using different ground impedance values under still air condition. In the 200Hz band, shown in Figure 8(a), the propagation is greatly attenuated by the ground effect and here we can see big differences between the predictions. The one using the range dependent ground impedance as derived from measurements agrees well with the measured SPL data, except that the measured levels spread over a significant range of values and the ground attenuation dip in the measured data is not as deep as that predicted by the BEM. This is to be expected since the measured data are affected by source level variations, atmospheric refraction and turbulence scattering, which are not accounted for in the BEM predictions. The prediction using the impedance obtained near the source agrees with the range dependent prediction well up to about 400m, where the impedance starts to change. From there on it differs and gives a slightly worse prediction than the range dependent prediction. The other two predictions using constant impedance values obtained at 500m and at 975m give significantly different predictions from the range dependent one and do not agree well with the measured SPL data. From prediction results over all the 1/3 octave bands from 100 to 400Hz in which ground attenuation has the most effect, it was found that, when used as a range independent value, the impedance measured at 975m is too soft and that measured at 500m is too hard for the prediction. This is in fact consistent with the ground parameter values shown in Table 1, and the visual observation that the ground at 500m is water logged. In the 500Hz frequency

band, Figure 8(b) shows that the sound propagation has largely recovered from the ground attenuation dip, and as expected there are only small differences between using range dependent and range independent ground impedance values. The dips at around 250m and 1179m are due to terrain screening rather than ground reflection attenuation.

This result show that, even for a generic grass cover field, range dependent ground impedance still plays an important part in determining the sound propagation within the frequency band where ground attenuation is most significant, which is typically from 100 to 400Hz.

(B) Range Dependent Sound Speed Profile

The raw wind and temperature data measured by the Sodar systems were merged with the temperature data into sound speed profiles. Since only one set of temperature profile measurements is available at the Metek position (1100m west of source), this set had to be used at all other locations. The merged sound speed profiles were then curve-fitted to provide smoothed profiles for input to the GTPE prediction program. Figure 9 shows an overview of the GTPE prediction in the 200Hz and 500Hz 1/3 octave bands over the entire 24 hour period of dataset 020821. The predictions used range independent sound speed profiles derived from the Metek Sodar wind and RASS temperature measurements at the single location of 1100m west of source. No turbulence is used in the prediction. It can be seen that the average trends follows the still air BEM predictions shown in Figure 8, showing that the GTPE calculation of ground terrain and impedance effects has accuracy compatible to that of the BEM, even for the complex terrain with impedance changes in this field trial. The predicted spread of sound levels due to changes in meteorological conditions throughout the 24 hour period also seems to match the spread in the measured data, although the overall mean levels in the prediction at locations around 250m and 1179m, which are positions shielded by the terrain geometry, are notably lower than the measured mean levels. This could be caused by range dependent meteorology or turbulence, both of which were not used in the predictions shown in Figure 9.

Figure 10 shows the smoothed profiles derived from the Metek measurement at 1100m and the AES Sodar measurements at 400m. Figure 10(a) shows the data at 22:03 while 10(b) shows the data at 21:01 hour on the next day. Some obvious differences can be seen especially in 10(b). The data suggest that the meteorology did change significantly along the propagation path, which is to be expected since the propagation is from a source at the bottom of a valley along the slope to the top of the hill. The significant changes in the sound speed profile are expected to have a large influence on the sound propagation. Figure 11 shows two sets of predictions in the 500Hz band - one using the Metek profile alone and the other using the AES profile alone. Predictions were made at six 150s time frames starting from 21:01 to show the possible effect of short term changes in the derived sound speed profiles. In Figure 11(a), it can be seen that the rather small gradient shown in the Metek profile in Figure 10(a) produced sound pressure levels that are largely similar to the still air values. On the other hand, in Figure 10(b), the negative gradient of the AES profile produced levels that are too low with obvious large shadows occurring at the longer distances. It should also be noted that the AES profiles generally produced much larger spreads than those produced by the Metek profiles. This reflects the large

variations in the raw data in 150s intervals. The question is whether Sodar measured data in short time intervals of 150s are reliable enough. Figure 10 also shows the profiles averaged over 25 minutes as broken lines. The longer time averaging produces profiles that are smoother and are apparently also more similar between the two locations. Figure 12(a) shows a prediction using the averaged AES Sodar profile alone, and Figure 12(b) shows a prediction using the averaged AES then the average Metek profile in the GTPE marching algorithm according to range, with a change-over distance set at 800m. The 25 minute averaging clearly eliminated the large spreads and shadows created by the variations in the 150s AES profile. The figure also shows that using range dependent profiles, in this case the AES profile (derived at 400m) for short range and the Metek profile (derived at 1100m) for range longer than 800m, improves the prediction significantly at range > 600m when compared with Figure 12(a). Generally using range dependent profiles seems to improve accuracy, but how to set the transition distance when only 2 profiles are available still needs further work to determine. Also it will be interesting to see if using the Lidar scanned profiles at every 100m interval will have a more significant effect. However the analysis of the Lidar data is taking more time than expected and the presentation of those results will be left to a future paper. Another point to be kept in mind when looking at these results is that, although the wind profiles were measured at different locations, temperature profiles were measured only at one location. This reduces the extent of the available range dependent meteorology data. Consequently it is expected that the range dependence of the derived sound speed profile is less than what actually occurred and the range dependent effect shown in the predictions should be considered as a lower estimate.

(C) Turbulence

The 1 dimensional isotropic turbulence parameters estimated from the single sonic anemometer measurements are rather small, as can be seen in Figure 7. As a preliminary investigation, GTPE predictions were performed using a simulated Gaussian turbulence spectrum with turbulence parameters typically used for low turbulence situations, i.e. refraction index fluctuation parameter $\mu^2=3x10^{-6}$ and length scale =1.1. A typical result is shown in Figure 13, which can be compared directly with the no-turbulence case shown in Figure 11(a). It seems that the effect of including this small turbulence is rather small except at range > 800m where the attenuation is reduced. It is however surprising to see that the effect is still small at the microphone position 1179m which is deep in the shadow zone of the hill top. A more detailed analysis of the derived turbulence parameters and the implementation of a more rigorous turbulence model will be needed to further examine the results.

VI. CONCLUSIONS

This paper presented the result of a field trail over a site with complex terrain features. The set of acoustic and meteorological data obtained is, we believe, more comprehensive than existing data that are available to public. The field trial implemented and tested the capability of a range of remote sensing meteorology measurement equipments in producing meteorological data for the study of acoustic propagation. It has been shown that sound speed profiles derived from these remote sensing measurements can produce reasonable predictions of the sound propagation and the spread of sound pressure levels measured in the field. The field trial also

performed ground impedance measurements at several locations. It shows that the method of short range excess attenuation and curve fitting using a 2 parameter model can provide reliable ground parameters that enable accurate predictions of ground effect, even on a field with difficult ground conditions.

On the subject of range dependence, it has been shown that it is essential to include range dependent ground data in the prediction of sound propagation. The inclusion of range dependent meteorology has also been shown to improve prediction accuracy although the conclusion is limited by the range independent temperature profiles used in the predictions.

Some limitations have also been found. The 150s measurement interval used by the remote sensing AES Sodar was found to produce too large a variation in the raw data to be reliable for acoustic predictions. A 25 minute averaging produces more consistent and reliable predictions. Due to the availability of equipment, temperature profiles were measured only at one location. This limits the extent to which the effect of range dependent meteorology has on sound propagation that can be studied. Also, the wind profiles measured by the Lidar system have not been implemented in the prediction simulations. Finally, the effect of turbulence, which is clearly seen in the measure data, has not been thoroughly analysed. These will be subjects of further research.

ACKNOWLEDGEMENTS

This research is funded by the UK Engineering and Physical Science Research Council under grant number GR/M71459. The authors would like to thank QinetiQ Ltd. for their collaboration in the work and for providing the site for the field trial, and the UK Royal Air Force for providing extra manpower and equipment for the field trial. The authors would also like to thank Prof. Stuart Bradley and Dr. Sabine von Hünerbein of the University of Salford for providing and operating the Sodar systems and subsequent analysis of the data, and Prof. Chris Collier, Dr. F. Davies, and Dr. K. E. Bozier of the University of Salford for providing and operating the Lidar system and subsequent analysis of the data.

REFERENCES:

1. M.E.Delany and E.N.Bazley, "Acoustical properties of fibrous absorbent materials", Applied Acoustics 3, 105-116, 1970.
2. K. Attenborough, "Models for the acoustical properties of the air saturated granular media," Acta Acust. 1, pp.213–226, 1993.
3. D. K. Wilson, D. I. Havelock, M. Heyd, M. J. Smith, J. M. Noble, and H. J. Auvermann, "Experimental determination of the effective structure-function parameter for atmospheric turbulence", J. Acoust. Soc. Am. 105 (2), pp.912-914 1999.
4. V. E. Ostashev, *Acoustics in moving inhomogeneous media*. E & FN Spon (an imprint of Thomson Professional), London, 1997.
5. E. M. Salomons, *Computational atmospheric acoustics*, Kluwer Academic Publishers, 2001.
6. Davies, F., Collier, C.G., Bozier, K.E., and Pearson, G.N., On the accuracy of retrieved wind information from Doppler lidar observations, Q. J. R. Meteorol. Soc.,129, 2003.
7. S. Taherzadeh and K. Attenborough, "Deduction of ground impedance from measurements of excess attenuation spectra", J. Acoust. Soc. Am. 105, pp.2039-2042, 1999.
8. R. A. Sack and M. West, "A parabolic equation for sound propagation in two dimensions over any smooth terrain profile: the generalised terrain parabolic equation (GT-PE)", Applied Acoustics 45, 113-129, 1995.
9. Y. W. Lam, "A boundary element method for the calculation of noise barrier insertion loss in the presence of atmospheric turbulence", Applied Acoustics 65(6), pp. 583-603, 2004.

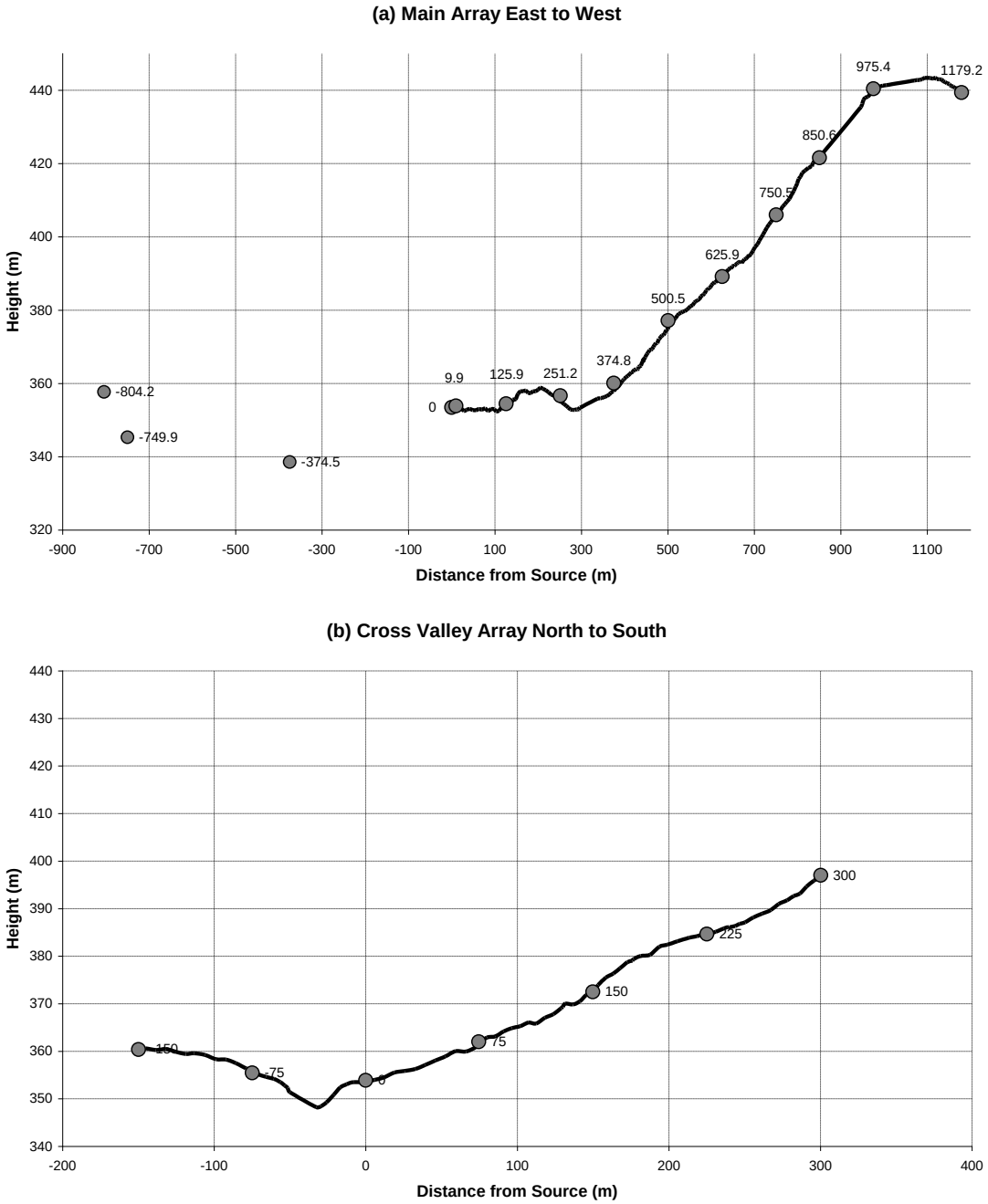

Figure 1 Ground Profile of the site, as measured by GPS approximately every 20m.

(a) 2 parameter ground model:

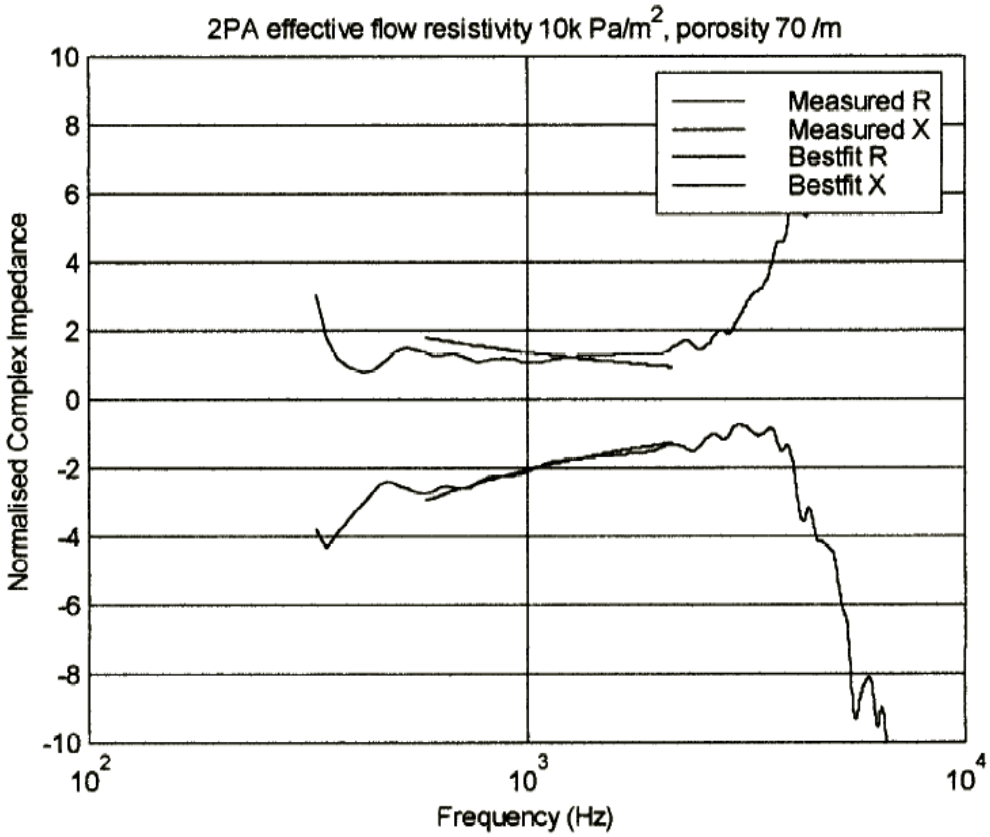

(b) Delaney and Bazley one parameter model:

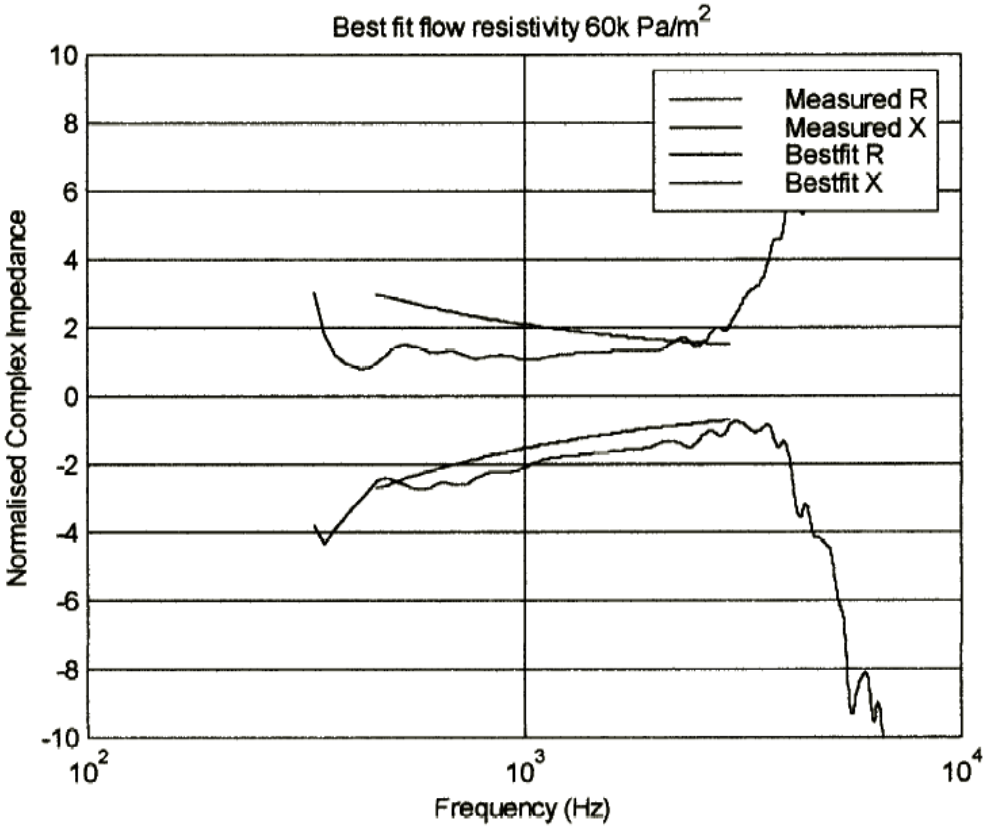

Figure 2 Typical best fits using different ground models to the impedance derived from measured short range excess attenuation spectra.

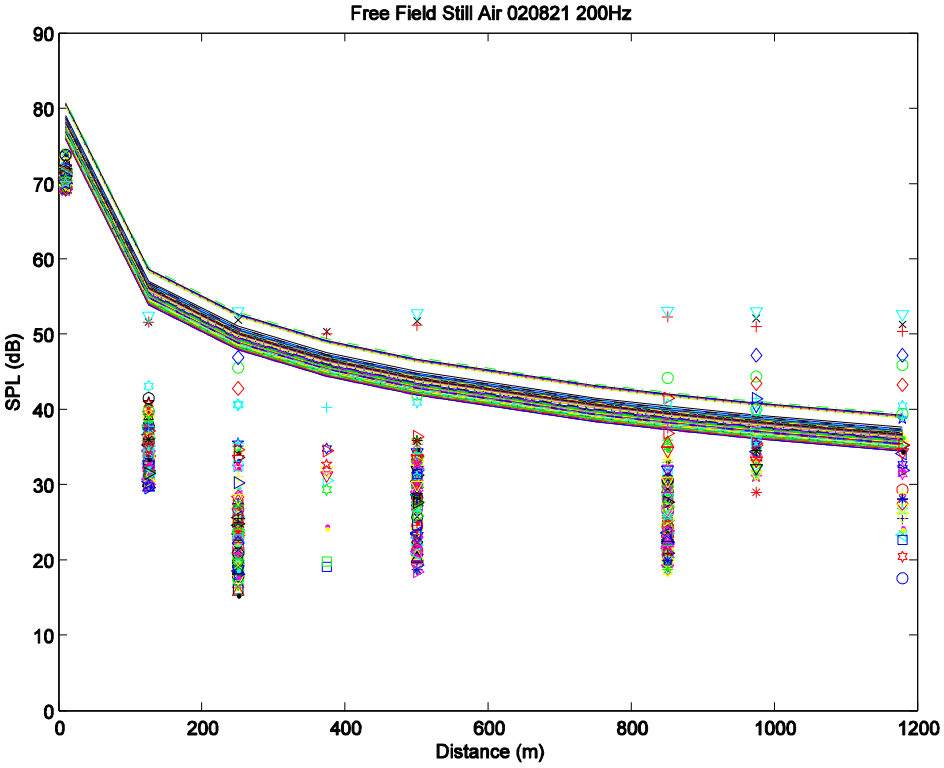

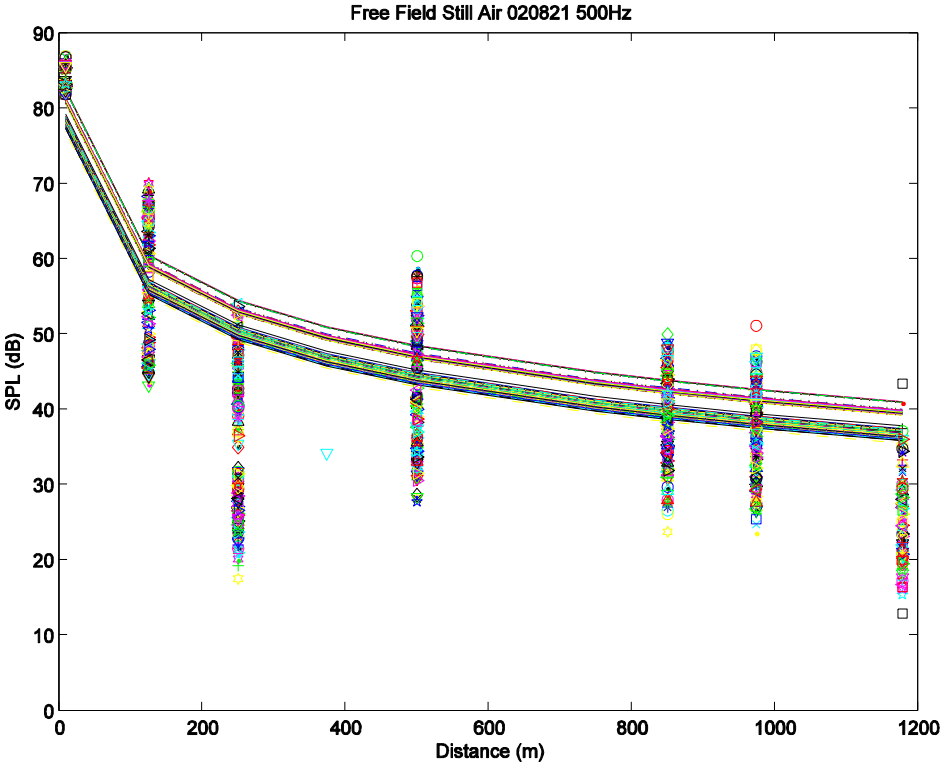

Figure 3 Sound pressure level along the main propagation path west of source in the 200Hz and 500Hz 1/3/ octave bands from dataset 020821. The different colours represent data from different time of the day within a 24 hour cycle. The solid lines are calculated free field values, which include adjustments for source power fluctuations.

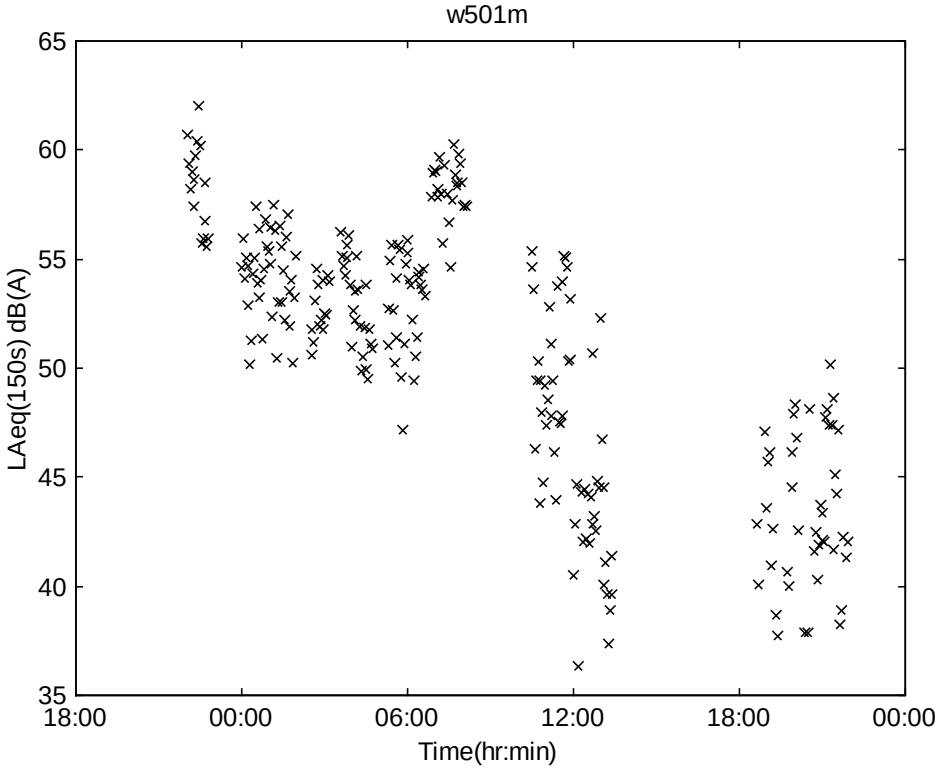

Figure 4 Variation of the L_{Aeq} sound pressure level at the 501m microphone position over the 24 hour period of the dataset 020821.

(a) Metek Sodar (green lines) and Lidar (blue lines) comparisons at 1100m west of source.

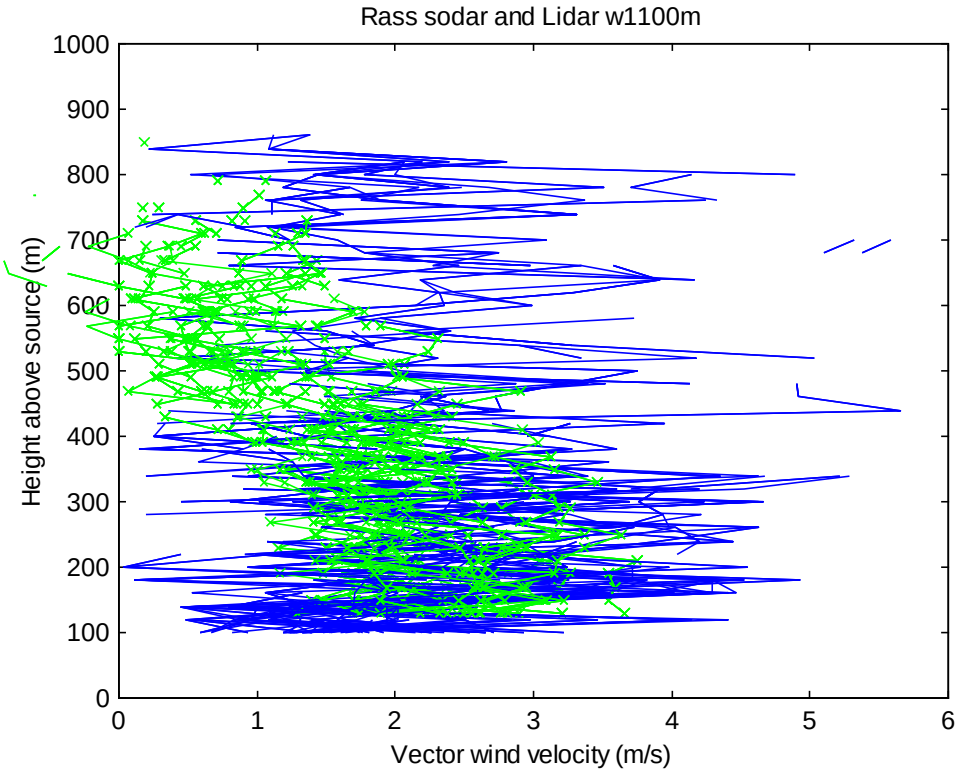

(b) AES Sodar (red lines) and Lidar (blue lines) comparisons at 478m west of source.

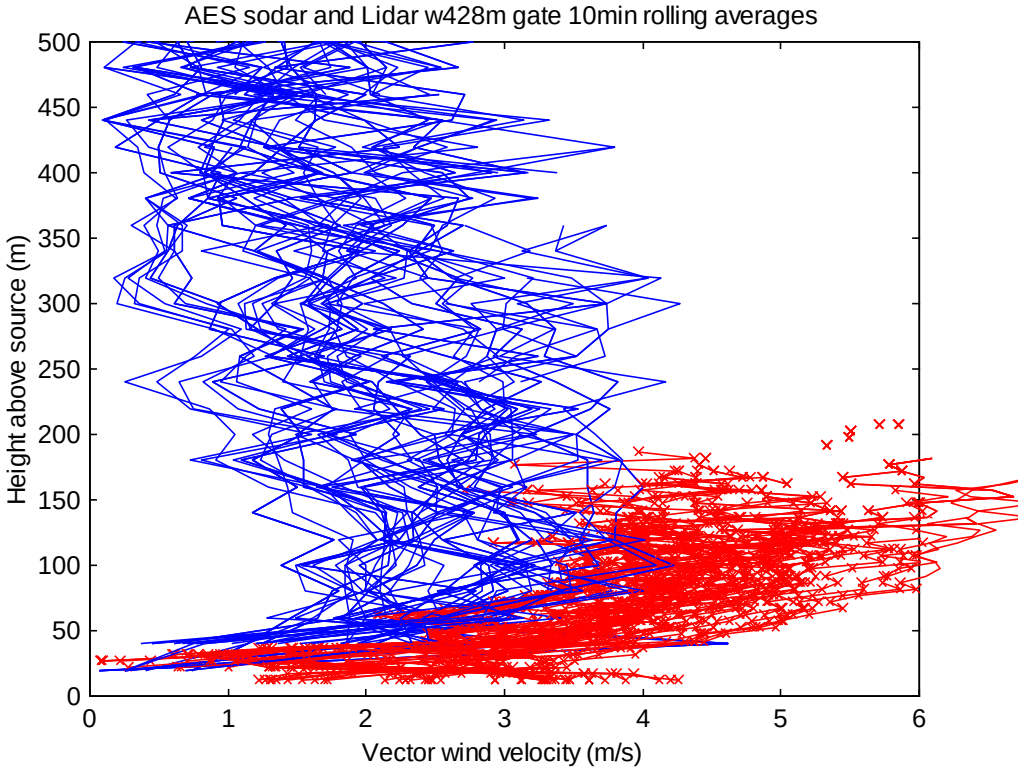

Figure 5 Overview of vector wind speed data derived from remote sensing equipments over the 24 hour cycle of dataset 020821.

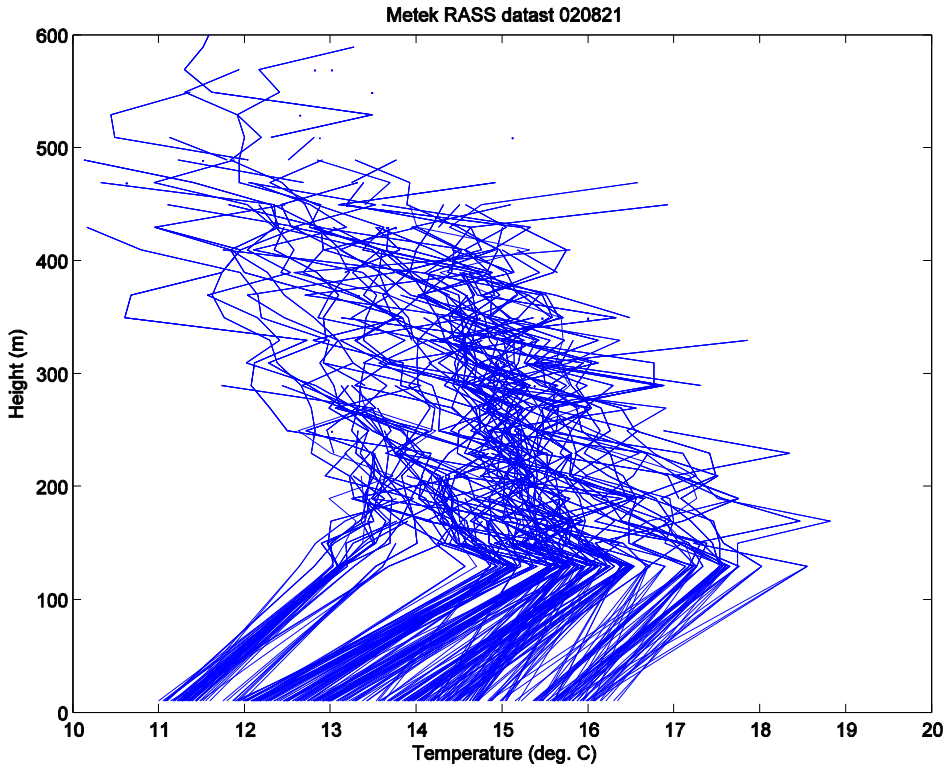

Figure 6 Temperature profiles derived from the Metek RASS system and sonic anemometer over the 24 hour period of dataset 020821.

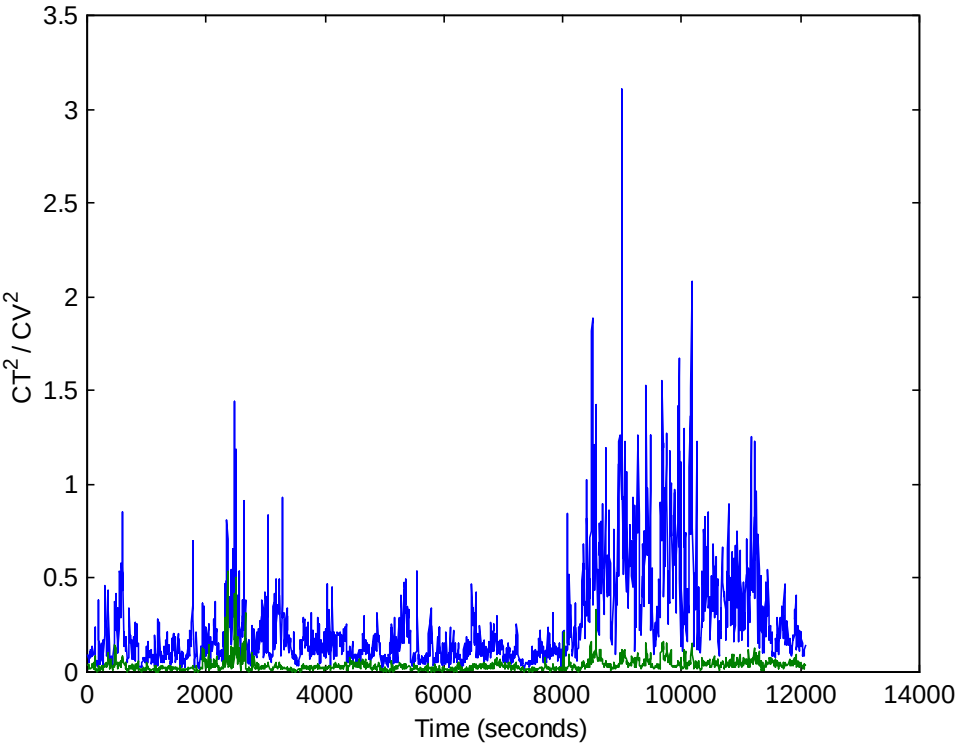

Figure 7 C_T^2 (green) and C_V^2 (blue) estimated from data measured by the Metek sonic anemometer.

(a)

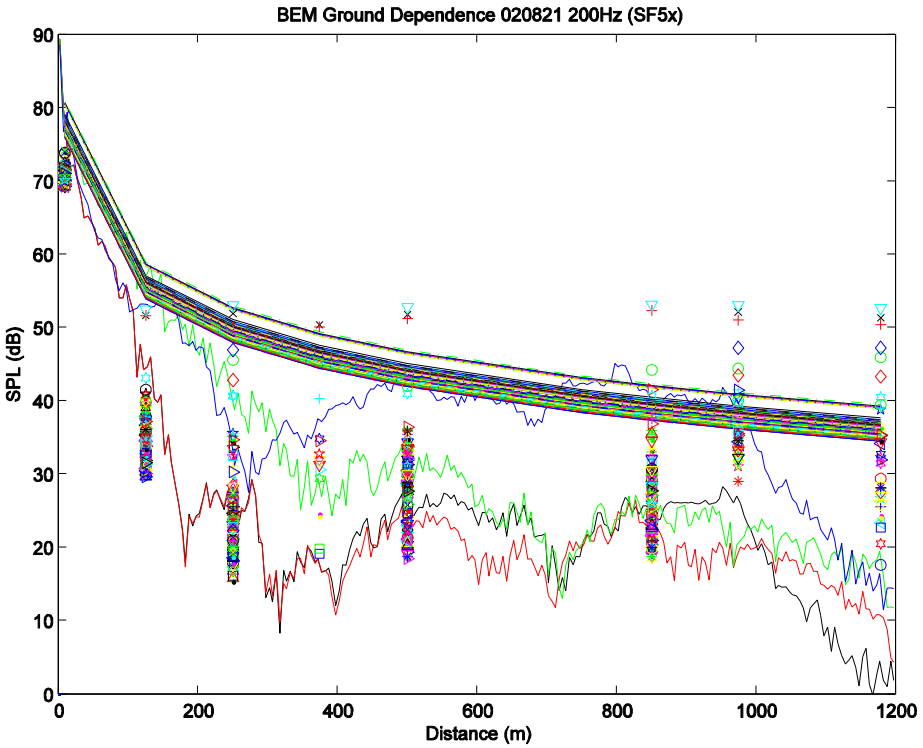

(b)

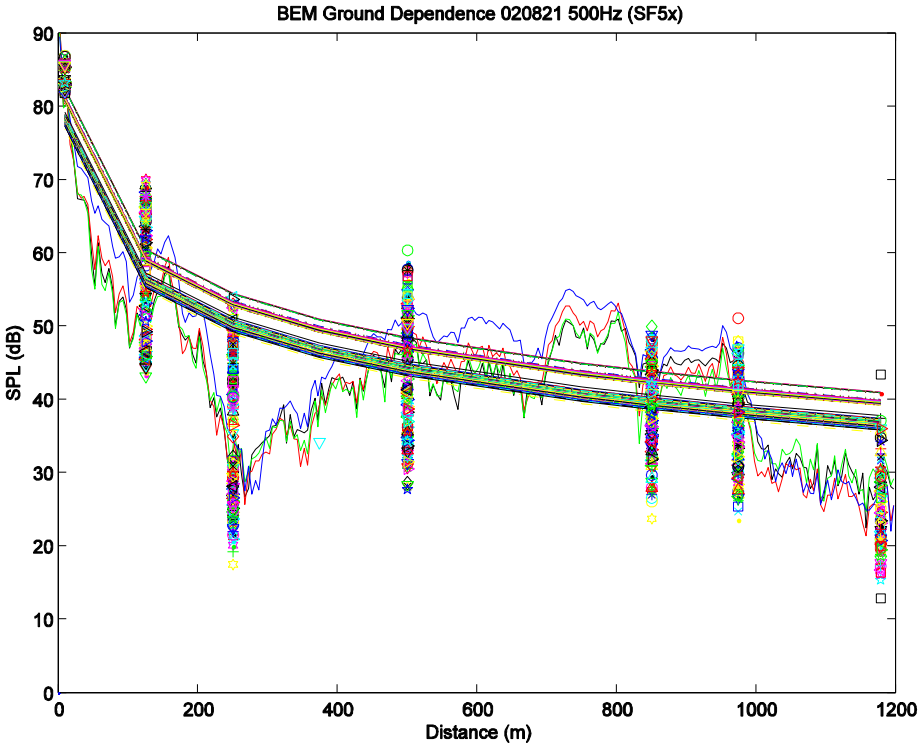

Figure 8 BEM prediction of sound propagation in still air, using range dependent ground impedance (black), constant impedance obtained near source (red), constant impedance obtained at 500m (green), and constant impedance obtained at 975m (blue). Symbols are measured SPL over 24 hour. The smooth lines are free field values showing the variation of source level during the measurement period.

(a)

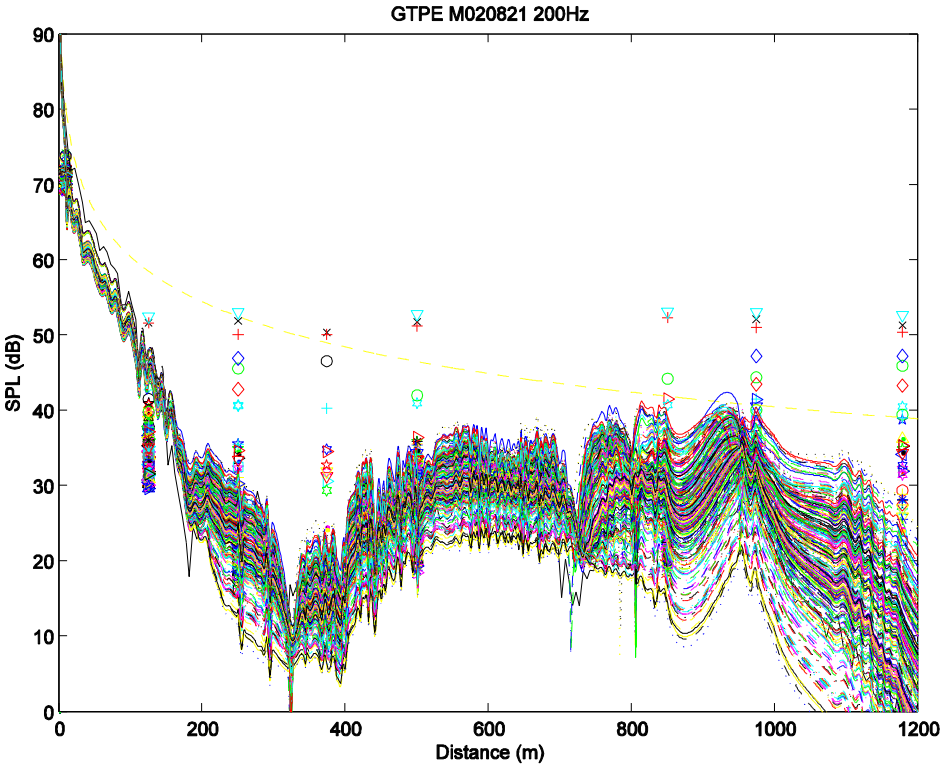

(b)

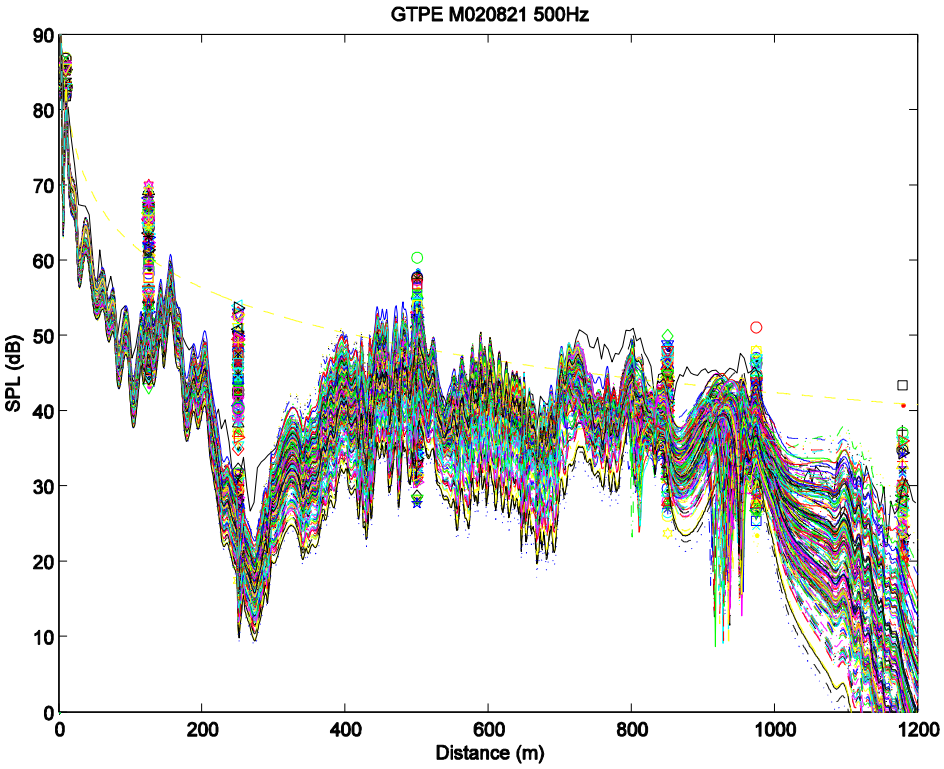

Figure 9 Overview of GTPE predicted sound propagation using the sound speed profiles derived from Metek Sodar and RASS measurements at 1100m west of source over the 24 hour period of dataset 020821.

(a)

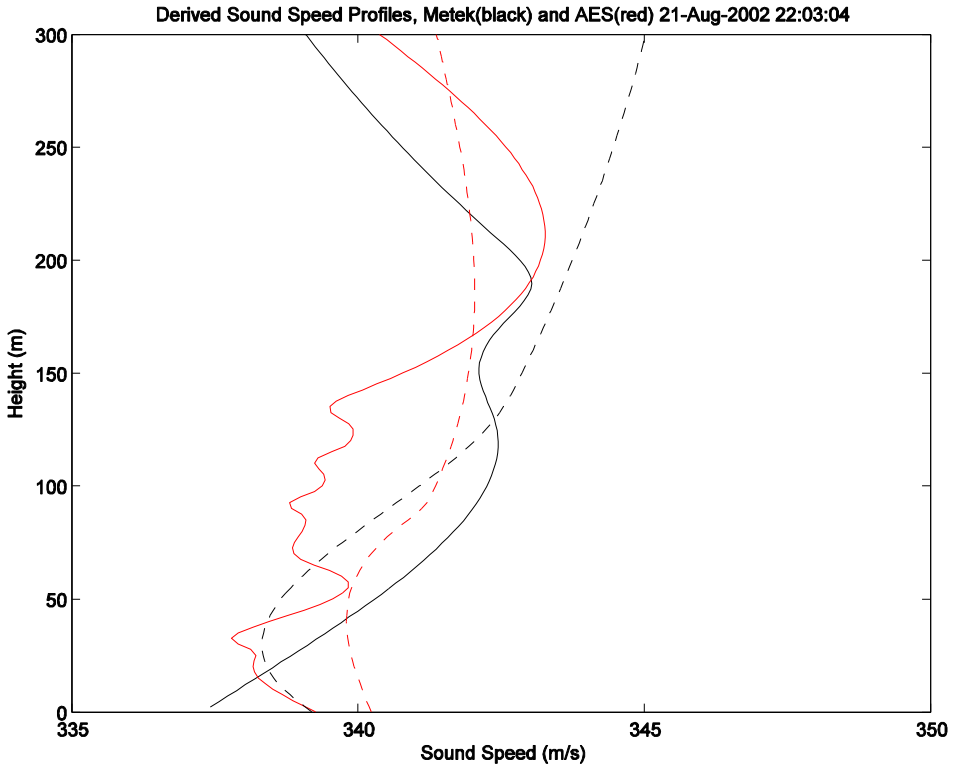

(b)

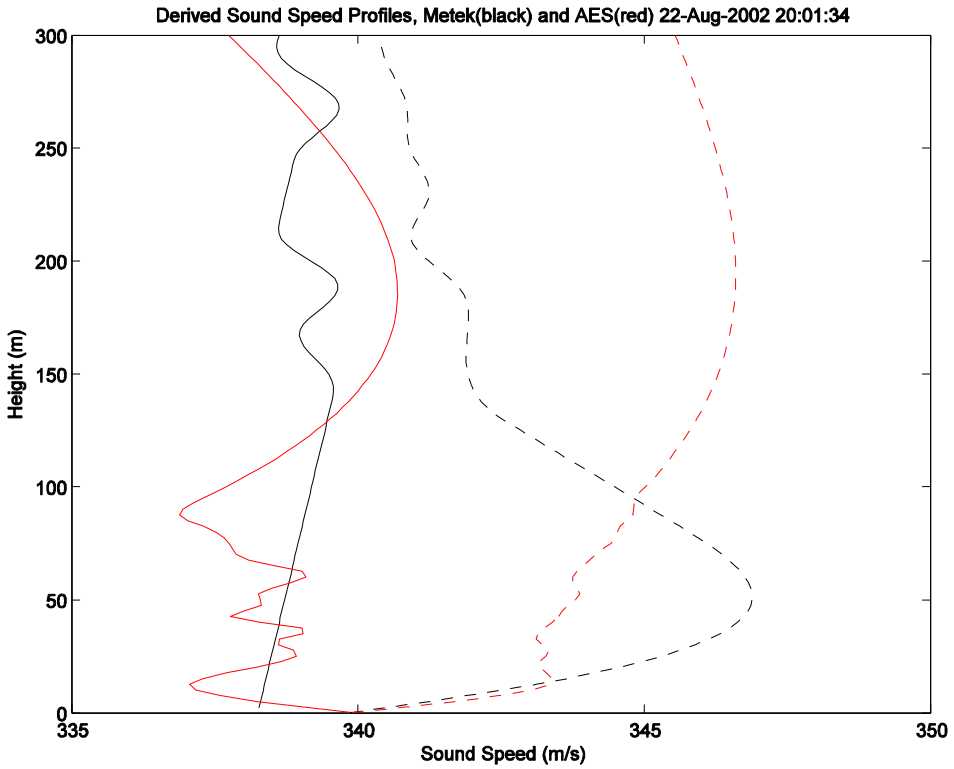

Figure 10 Smoothed sound speed profiles from Metek (black) and AES (red) Sodar measurements. Solid lines are 150s samples. Broken lines are 25 minute samples.

(a) Using Metek derived 150s sound speed profiles (1100m west of source)

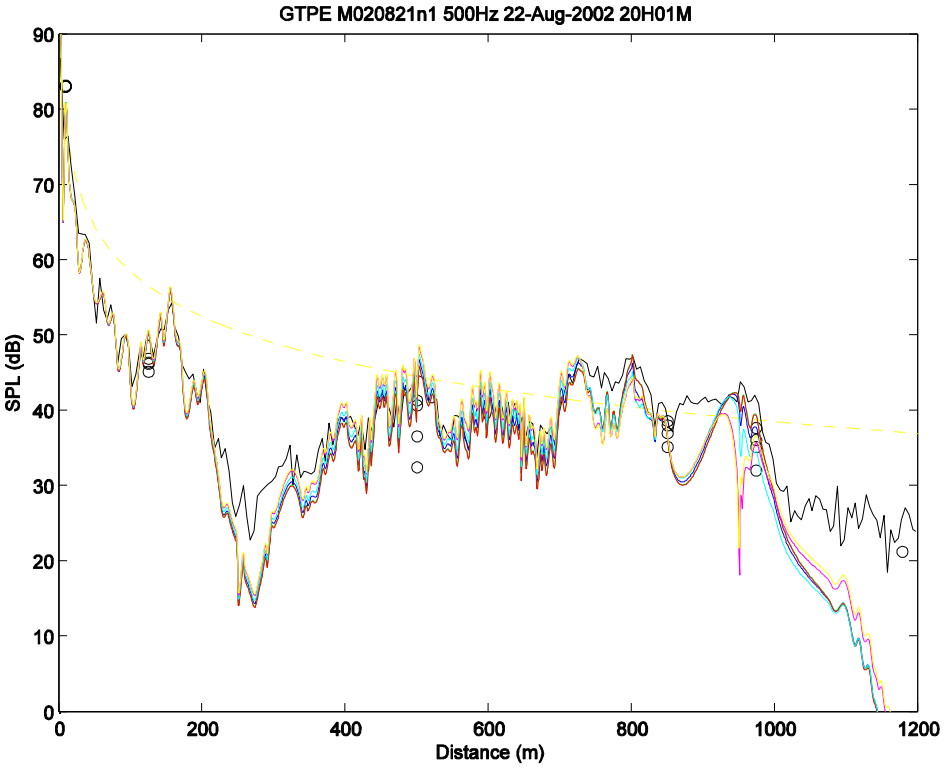

(b) Using AES derived 150s sound speed profiles (400m west of source)

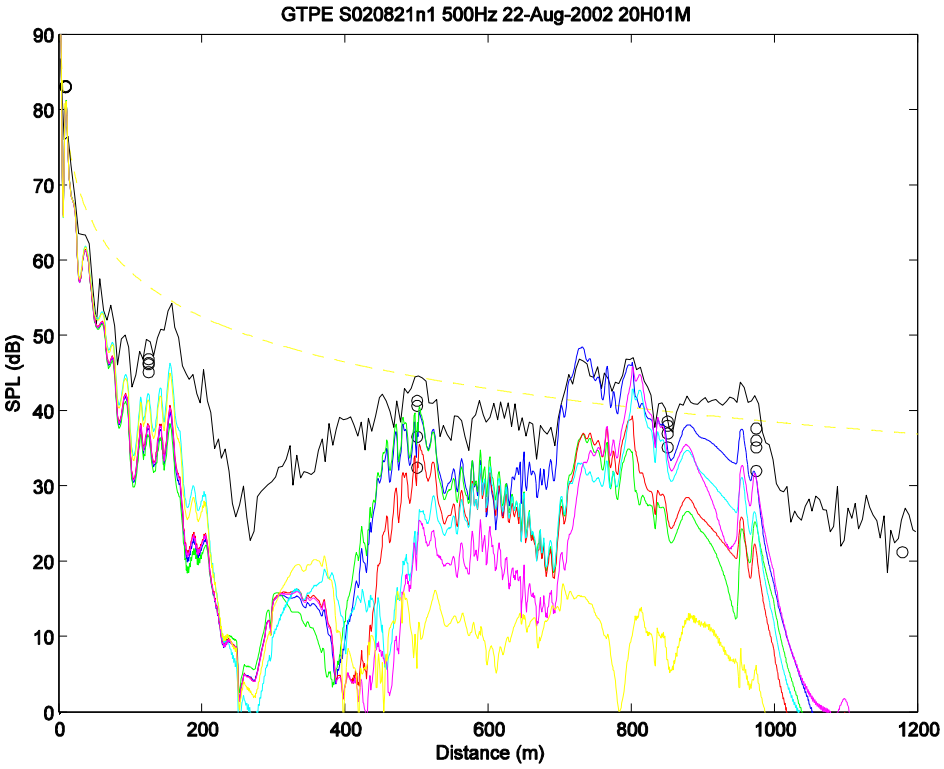

Figure 11 GTPE predictions at 500Hz using two sets of range independent sound speed profile in six 150s intervals starting from 20:01. Black solid line is BEM still air prediction.

(a) Prediction using the 25 minute averaged AES profile

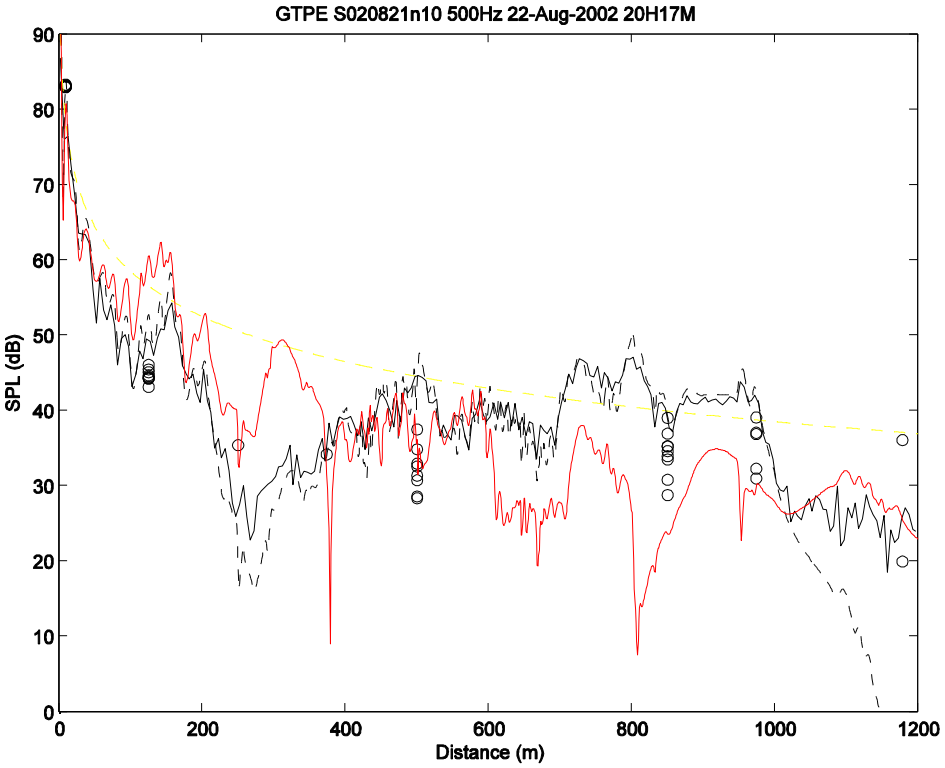

(b) Range dependent prediction using 25 minute averaged AES & Metek profiles

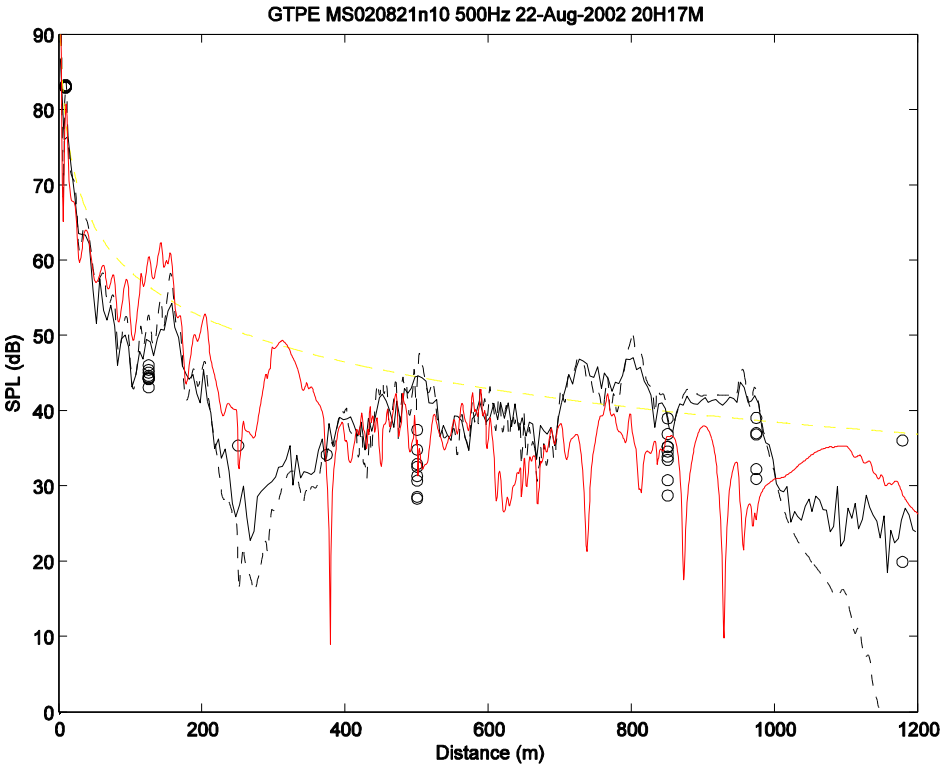

Figure 12 GTPE predictions (red) using 25 minute averaged sound speed profiles. (a) is range independent using AES profile. (b) is range dependent using both AES and Metek profiles. Black lines are still air predictions – solid line is BEM and broken line is GTPE.

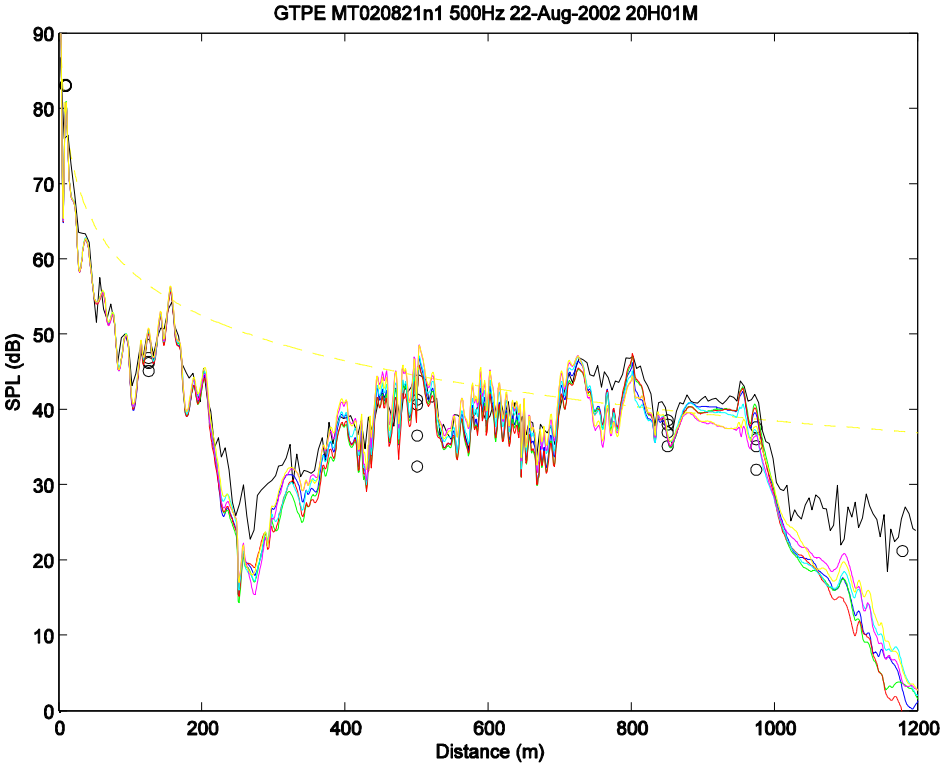

Figure 13 GTPE prediction for the same situation as in Figure 11(a) but with small turbulence included.